Check for updates

Changes of phase composition of maraging steel 1.2709 during selective laser melting

Miroslav Mashlan[1] · Fredericus Linderhof[1] · Magdalena Davidova[1] ·
Hana Kubickova[2] · Elena Zemtsova[3]

Abstract

Selective laser melting (SLM) as an additive manufacturing technology enables the quick production of complex shaped three-dimensional (3D) specimens directly from a metal powder. Various metal powders, including different steels, are used in this technology. The influence of the SLM process on the phase composition of the final 3D specimen has been examined by Mössbauer spectroscopy (MS) The surface quality has been examined by scanning electron microscopy (SEM) and energy-dispersive X-ray spectroscopy (EDS). The maraging steel 1.2709 (CL50WS), an iron-nickel steel alloy, which is often used in applications where high fracture toughness and strength are required has been investigated. The difference between the phase composition of the initial CL50WS powder and the final specimen identified via MS demonstrated transformation of a martensitic phase into an austenitic one. This transformation proceeds during the whole SLM process. SEM presented imperfections of the surface of the final specimen. The spherical and irregular pores were observed as well as the particles of initial powder bonded to face. Inhomogeneity of elements on the face has been observed by EDS.

Keywords Maraging 1.2709 · Selective laser melting · Martensite · Austenite · Mössbauer spectroscopy · Scanning electron microscopy · Energy-dispersive X-ray spectroscopy

---

✉ Miroslav Mashlan
miroslav.maslan@upol.cz

1   Faculty of Science, Palacky University, Olomouc, Czech Republic

2   Science and Technology Park of Palacky University, Olomouc, Czech Republic

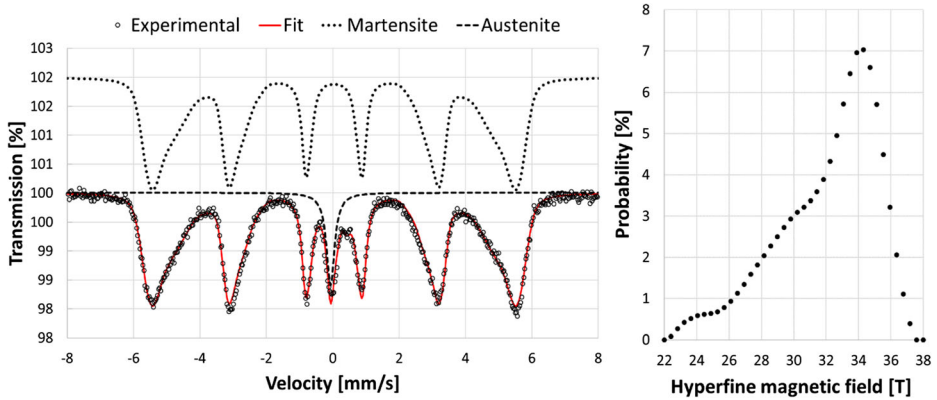3   Saint Petersburg State University, Saint Petersburg, Russia

Fig. 1 RT Mössbauer spectrum of the CL50WS powder (left) and distribution of magnetic fields of martensite (right)

1 Introduction

Selective laser melting (SLM) is probably the most rapidly growing technique in additive manufacturing (AM) technologies. The laser selectively melts the powdered material by scanning cross-sections on the surface of a powder bed in accordance to a 3-D digital description of the required component. After each cross-section is scanned, the powder bed is lowered by one layer of its thickness. A new layer of material is applied on the top and the process is repeated until the component is completed [1–3]. To date the main objective in the SLM field is to produce components with mechanical features comparable with those produced with traditional techniques. These properties depend on composition and size of the powder granules as well as on the process parameters. The SLM process has proved to be suitable for manufacturing hard tool steels, stainless steels, various metal composites, Ni, Ti, and Mg alloys. The optimization of process parameters and studying the microstructure of final components, their tensile tests and the hardness and roughness characterization has been discussed in many papers [4–6]. Although Mössbauer spectroscopy (MS) is an excellent tool for examining iron based components, no paper has been devoted to the study of the components and their face manufactured by SLM via MS. The objective of this work is to investigate experimentally the face of components manufactured via the SLM process using MS, scanning electron microscopy (SEM), and energy-dispersive X-ray spectroscopy (EDS).

Table 1 Chemical composition of the CL50WS steel powder

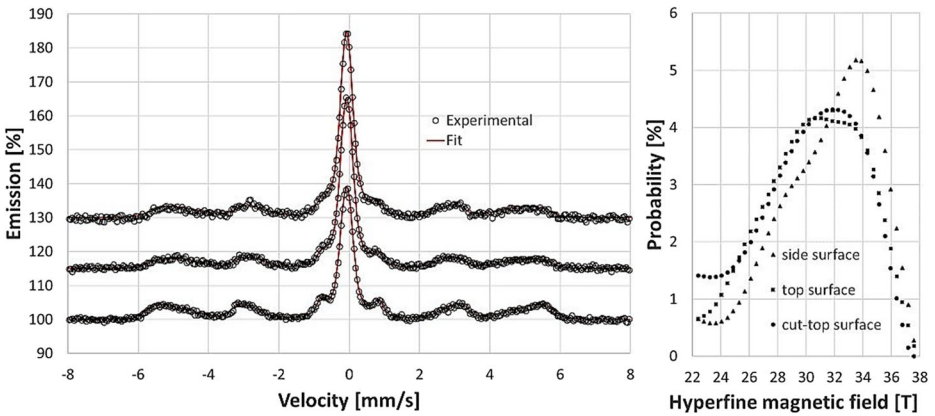| Element concentration, wt%								
Fe	C	Si	Mn	Cr	Mo	Ni	Ti	Co
Balance	≤ 0.03	≤ 0.10	≤ 0.15	≤ 0.25	4.50–5.20	17.0–19.0	0.80–1.20	8.50–10.0

Fig. 2 The backscattering Mössbauer spectra (left) measured on the side face (bottom), top face (central) and cut-top face (upper). Distribution of hyperfine magnetic fields on different faces (right)

2 Materials and methods

The CL50WS powder of the iron-nickel steel alloy (hot-work steel 1.2709) with the chemical composition presented in Table 1 was used for making the test sample by SLM and annealing the CL50WS powder at different temperatures.

The scanning electron microscope VEGA3 LMU with secondary electron detector of the Everhart-Thornley type (TESCAN, Brno, Czech Republic) and XFlash silicon drift detector 410-M (Bruker Nano GmbH, Berlin, Germany) were used for imaging of CL50WS powder, the faces of the final component, and also for elemental analysis by EDS.
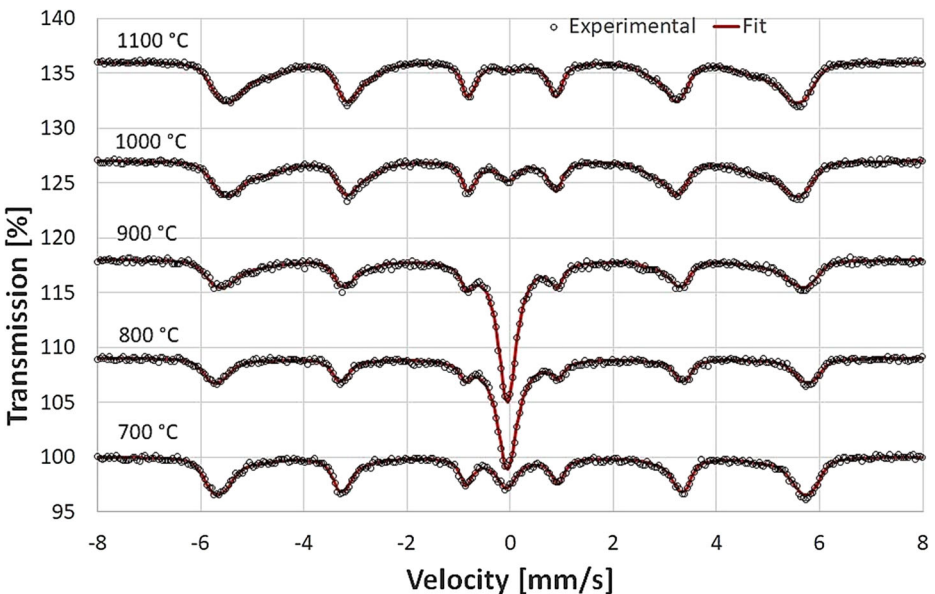

Fig. 3 The RT Mössbauer spectra of the CL50WS powder after annealing at different temperatures

Table 2 Subspectra areas

subspectra area	austenite	martensite
initial powder	9 ± 1	91 ± 1
side face	45 ± 1	55 ± 1
top face	59 ± 1	41 ± 1
cut top face	58 ± 1	42 ± 1

Transmission and backscattering ^{57}Fe Mössbauer spectra were measured by a system employing a MS96 Mössbauer spectrometer [7] operating in a constant acceleration mode and equipped with a ^{57}Co(Rh) source. The SiLi detector which registers 14.4 keV gamma ray was used for the accumulation of backscattering spectra. The acquired Mössbauer spectra were evaluated using the MossWinn software program [8]. The isomer shift values were referred to the centroid of the spectrum recorded from an α-Fe foil (thickness 30 μm) at room temperature.

The Nabertherm furnace with B130 controller (Nabertherm GmbH, Germany) was used to anneal the CL50WS powder at the 700–1100 °C temperature range in an argon atmosphere.

3 Experimental

A testing sample of prim form was obtained by SLM on the Concept Laser M2-cusing system. The system was equipped with a Yb:YAG diode-pumped fibre-optical laser whose power and wavelength were 400 W and 1070 nm, respectively. Synthesis was performed using mode with power 200 W and a scanning rate of 1600 mm/s. The testing sample was cut up to two half prism in a parallel plane to the top face (relative to building direction) by hacksaw and the new originated face (cut-top face) was investigated. The backscattering Mössbauer spectra of the testing sample were measured on the top and side faces (relative to building direction) as well as on the cut-top face. The quality of the surfaces was examined by SEM, which allows observing the morphology difference for various faces. The distribution of elements on the faces was studied by EDS. A complementary study of the CL50WS powder behavior after annealing at different temperatures was carried out. The CL50WS powder was annealed at different temperatures in an argon atmosphere by the following time scheme: heating from
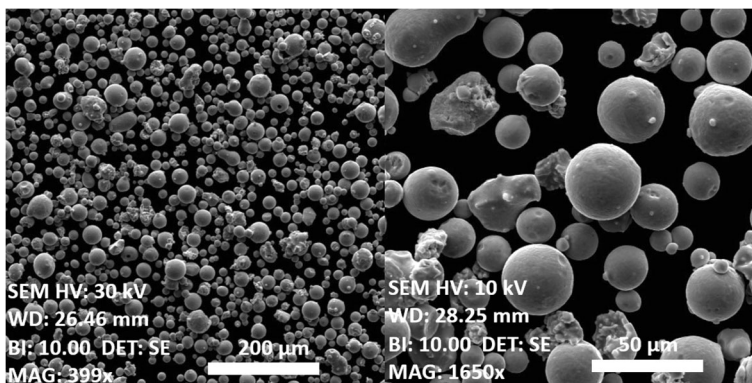

Fig. 4 Morphology of the CL50WS powder used for SLM

Table 3 The RT Mössbauer parameters of the initial and annealed CL50WS powder (IS – isomer shift, B – hyperfine magnetic field, FWHM - full width at half maximum, A – subspectrum area)

sample	austenite			martensite		
	IS [mm/s]	FWHM [mm/s]	A [%]	IS [mm/s]	B [T]	A [%]
CL50WS initial	−0.07	0.37	9	0.01	32.3	91
CL50WS annealed at 700 °C	−0.07	0.48	14	0.04	34.4	86
CL50WS annealed at 800 °C	−0.06	0.45	50	0.03	34.8	50
CL50WS annealed at 900 °C	−0.08	0.42	44	0.01	33.6	56
CL50WS annealed at 1000 °C	−0.05	0.44	7	0.03	32.7	93
CL50WS annealed at 1100 °C	−0.05	0.53	3	0.04	32.8	97

room temperature to the final temperature for 0.5 hour – annealing at the final temperature for 1 hour – spontaneously cooling to room temperature for approximately 8 hours. The transmission Mössbauer spectra were obtained for the samples annealed at 700, 800, 900, 1000, and 1100 °C.

4 Results and discussion

4.1 Mössbauer spectroscopy

The Mössbauer spectrum of the CL50WS powder was recorded in a transmission mode at room temperature (RT). The RT Mössbauer spectrum of the CL50WS powder was analyzed as a combination of singlet corresponding to austenite and distribution of hyperfine magnetic field corresponding to the ferrite phase (martensite) (Fig.1 and Table 3). The austenite phase was identified in the Mössbauer spectrum of CL50WS (hot-work steel 1.2709, maraging steel) powder. This fact is in contradiction with the reported Mössbauer spectra of the hot-work steel 1.2709 (maraging steel) [9–11], where no austenite was identified.

The backscattering Mössbauer spectra of the testing sample were measured on the top, side, and cut-top faces (Fig.2, left). The different subspectra areas are presented in Table 2. We can see that the contribution of austenite in the testing sample is approximately five times higher than in the initial powder. There is a difference in the austenite/martensite ratio determined from the Mössbauer spectra obtained on the side and top faces. This difference is probably connected with welding the initial particles on the surface which is confirmed by the SEM
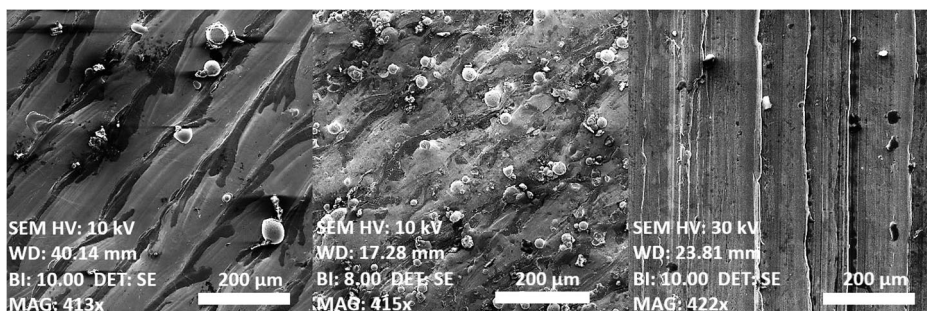

Fig. 5 SEM images of the top face (left), side face (center) and cut-top face (right)
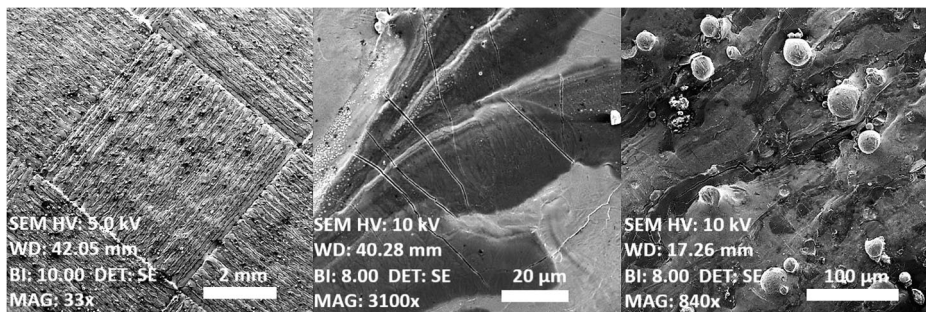
Fig. 6 SEM images of the top face with identification of the laser beam motion (left), detail of top face (center) and side face (right) with micro scratches

images (see paragraph 4.2). The influence of welding initial particles on the Mössbauer spectra is also demonstrated by the distribution of hyperfine magnetic field (Fig.2, right). The hyperfine magnetic field distribution for the side face spectrum is different from those for the top and cut-top face spectra and, consequently, is similar to the hyperfine magnetic field distribution of CL50WS particles.

The obtained Mössbauer spectra of the CL50WS powder after annealing at different temperatures are presented in Fig. 3. The RT Mössbauer parameters and content of austenite and martensite are given in Table 3. It can be seen that the most intensive transformation from martensite into austenite occurs at the temperatures around 800 °C. The same transformation was observed after annealing at 650 °C for 12 hours with plates of magraging-350 steel prepared by rolling via Mössbauer spectroscopy and was confirmed by X-ray diffraction [9].

4.2 Scanning electron microscopy

SEM was use to characterize the morphology and size of particles of the initial CL50WS powder. Images of separate granules of initial CL50WS powder are presented in Fig. 4. The granule sizes are dominantly in the interval between 10 and 20 μm. The differences of quality of various faces were observed by SEM (Fig. 5). Particles of CL50WS powder are welded on the top and side face. The number of welded particles on the side face was greater than on the top one, as the side face was in contact with CL50WS powder during SLM process whereas the top face was in contact with an inert atmosphere. At the same time it was observed that the roughness on the side face was greater than on the top face. The lighter and darker trails on the top face image were in compliance with the direction of the motion of the laser beam Fig. 6, left). The microscratches were identified when
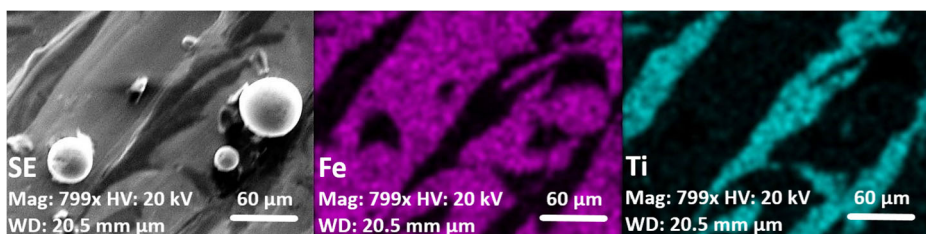

Fig. 7 Element distribution on the top face: SEM image (left), Fe (center) and Ti (right) distributions
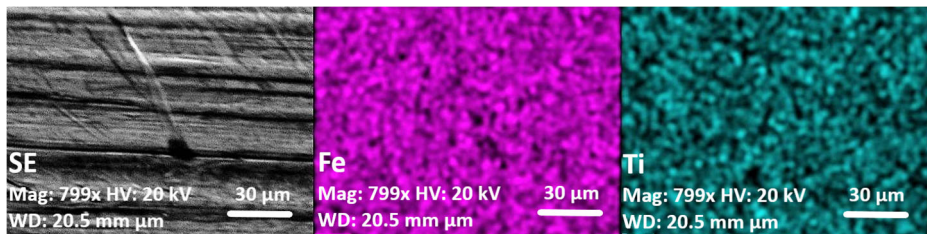
Fig. 8 Element distribution on the cut-top face: SEM image (left), Fe (center) and Ti (right) distributions

applying greater magnification on the top and side faces (Fig. 6, centre, right). Commonly the face of the components prepared by SLM are treated for better roughness by cutting or jetting. The quality of the face after cutting is demonstrated in Fig. 5 (right) where we can see lines corresponding to the cut direction.

4.3 Energy-dispersive X-ray spectroscopy

The lighter and darker trails on the top face image, less intensive on the side face, were observed. EDS identified an interesting distribution of elements. The lighter trails refer to more intensive identification of iron (Fig. 7 centre), nickel, cobalt, and molybdenum (not demonstrated as the images are similar to iron). On the other side, more intensive identification of titanium corresponds to the darker trails (Fig. 7 right). This separation of titanium was observed only on the top and side faces. The homogenous distribution of all elements (Fe, Ni, Co, Mo, Ti) was identified on the face after cutting (Fig. 8).

5 Conclusions

Transformation of the martensitic phase into austenite phase has been observed by MS. This transformation proceeds during the SLM process and is related to the products temperature that is kept in the range of 800 °C for a relatively long time. Transformation of the martensite into austenite during SLM process was confirmed by the CL50WS powder annealing at the temperature interval 800–900 °C. This transformation does not occur at lower temperatures and the opposite transformation starts at the temperature higher than 1000 °C. Different ratio between austenite and martensite phases for different faces of the product could be explained by the initial powder particles welding. The existence of inhomogeneity in the distribution of different elements on the face was observed by EDS. The face of the product can be cleaned from the element inhomogeneity as well as the welded particles by cutting or jetting.

References

1. Kruth, J.P., Froyen, L., Van Vaerenbergh, J., Mercelis, P., Rombouts, M., Lauwers, B.: Selective laser melting of iron-based powder. J. Mater. Process. Technol. **149**, 616–622 (2004)
2. Frazier, W.E.: Metal additive manufacturing: a review. J. Mater. Eng. Perform. **6**(23), 1917–1928 (2014)
3. Afkhami, S., Dabiria, M., Alavib, S.H., Björka, T., Salminenc, A.: Fatigue characteristics of steels manufactured by selective laser melting. Int. J. Fatique. **122**, 72–83 (2019)
4. Al-Ketan, O., Rowshan,, R., Abu Al-Rub, R.K.: Topology-mechanical property relationship of 3D printed strut, skeletal, and sheet based periodic metallic cellular materials. Addit. Manufact. 19, 167–183 (2018)
5. Patel, C.M., Patel, S.B., Shah, M.K.: Experimental investigation of mechanical properties and surface roughness of CL50WS material parts made by selective laser sintering process. Int. J. Sci. Res. Dev. **3**, 306–310 (2015)
6. Jägle, E.A., Sheng, Z., Kürnsteiner, P., Ocylok, S., Weisheit, A., Raabe, D.: Comparison of Maraging steel micro- and nanostructure produced conventionally and by laser additive manufacturing. Materials. **10**, 1–15 (2017)
7. Pechousek, J., Mashlan, M.: Mössbauer spectrometer as a virtual instrument in the PXI/compact PCI modular system. Czechoslov. J. Phys. **55**, 853–864 (2005)
8. Klencsár, Z., Kuzmann, E., Vértes, A.: User-friendly software for Mössbauer spectrum analysis. J. Radioanal. Nucl. Chem. **210**, 105–118 (1996)
9. Nunes, G.C.S., Sarvezuk, P.W.C., Alves, T.J.B., Biondo, V., Ivashita, F.F., Paesano Jr., A.: Maraging-350 steel: following the aging through diffractometric, magnetic and hyperfine analysis. J. Magn. Magn. Mater. **421**, 457–461 (2017)
10. da Silva, J.J.M., de Vasconcelos, I.F., da Silva, F.I.S., Ribeiro, T.S., de Abreu, H.F.G.: An atomic redistribution study of the 440°C ageing kinetics in maraging-300 steel. Mater. Res. **22**(1), e20180230 (2019)
11. Alves, T.J.B., Nunes, G.C.S., Sarvezuk, P.W.C., Ivashita, F.F., Andrade, A.M.H., Viegas, A., Paesano Jr., A.: Crystallographic, hyperfine and magnetic characterization of a maraging-400 alloy. Hyperfine Interact. **238**, 45 (2017)